

RELATIONSHIPS AMONG SOME
LOCALLY CONSERVATIVE
DISCRETIZATION METHODS
WHICH HANDLE DISCONTINUOUS
ANISOTROPIC COEFFICIENTS
ON DEFORMED GRIDS

Thomas F. Russell
National Science Foundation

Joint work with:

Runhild Klausen, Ragnar Winther
University of Oslo

Richard Naff, John Wilson
U.S. Geological Survey

Funding support: NSF, WES/ARO, USGS

Similarity between different discretization methods for

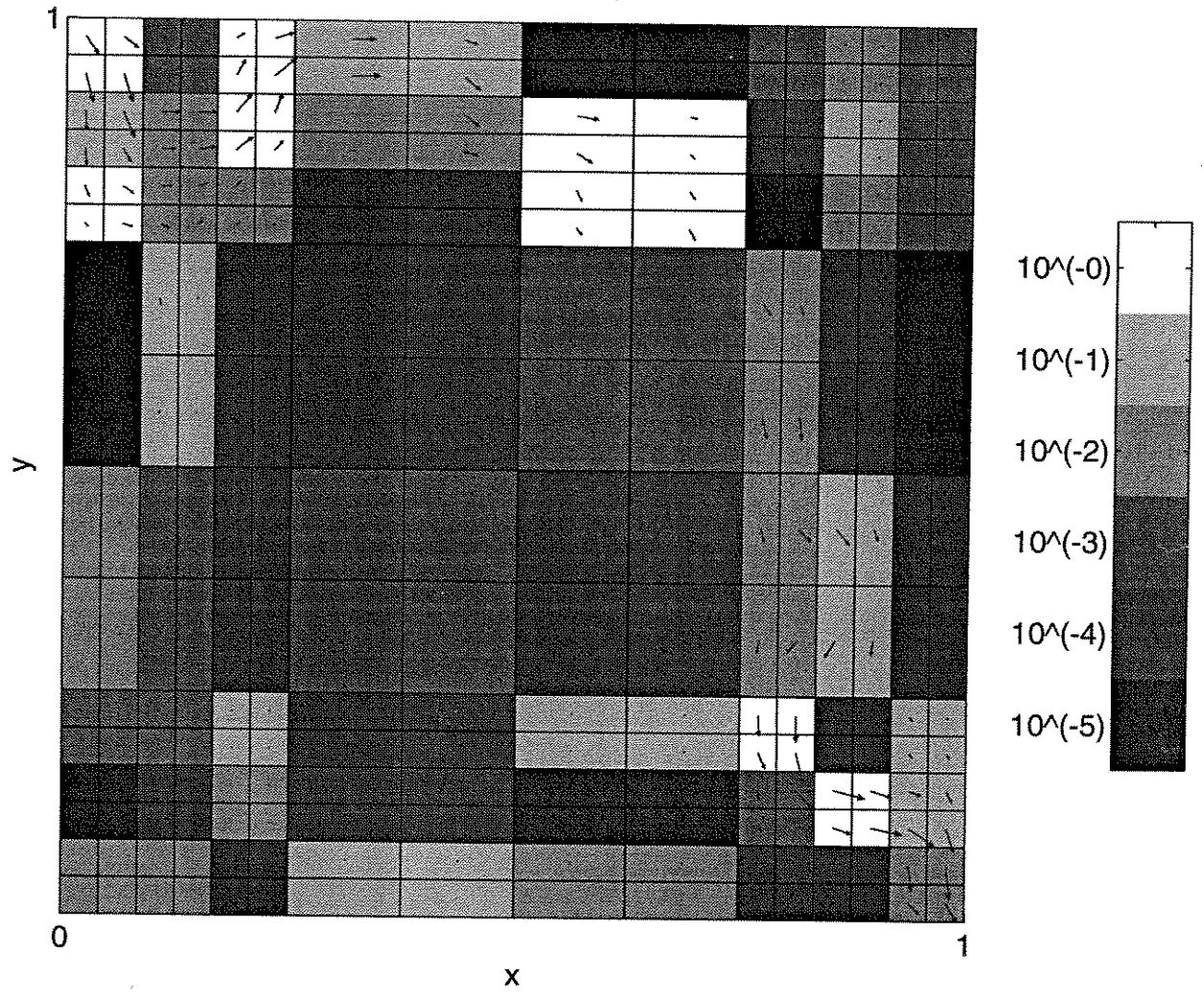
$$\begin{aligned} -\operatorname{div}(\mathbf{K}(\mathbf{x})\operatorname{grad} p) &= g \text{ in } \Omega, \\ p(\mathbf{x}) &= 0 \text{ on } \partial\Omega, \end{aligned}$$

- General irregular grid,
- Anisotropic permeability, and
- Heterogeneous discontinuous permeability
 $\implies \operatorname{grad} p = 1\text{-form}$ (tangential continuity)
 $\mathbf{K} \operatorname{grad} p = 2\text{-form}$ (normal continuity)

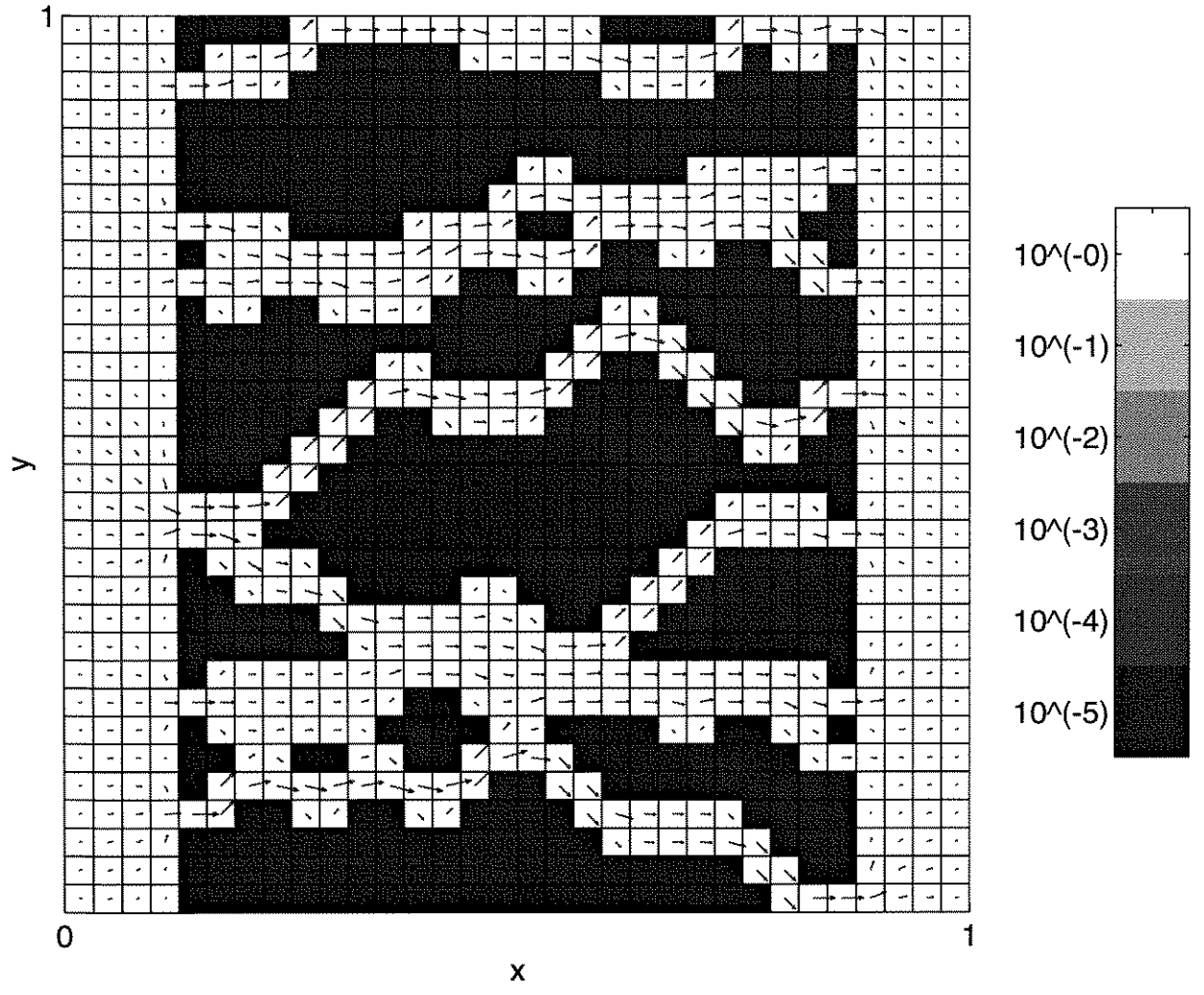
What types of methods are well suited and why?

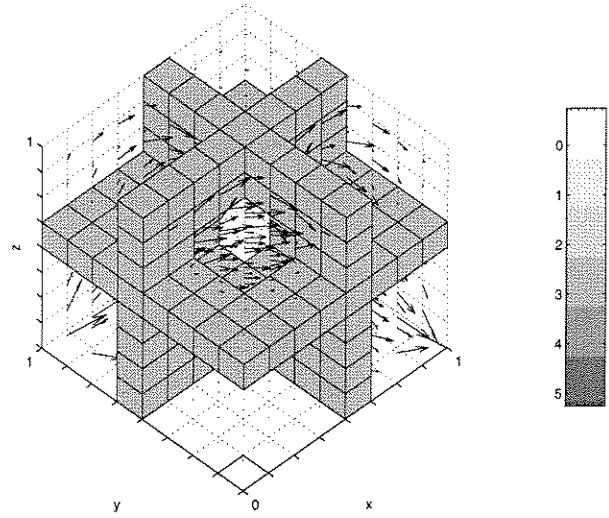
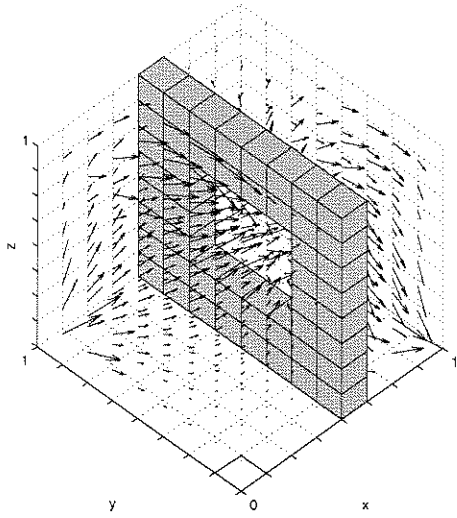
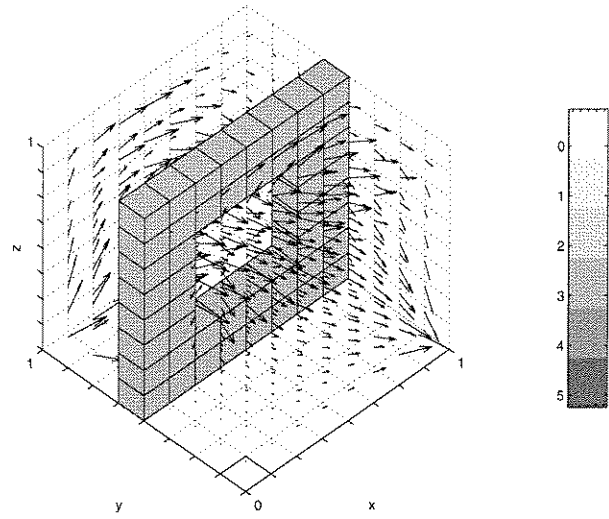
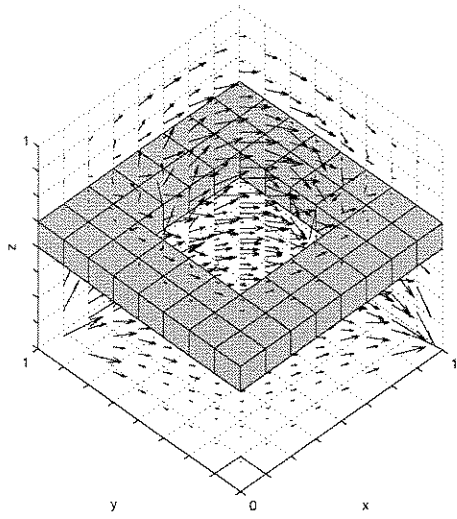
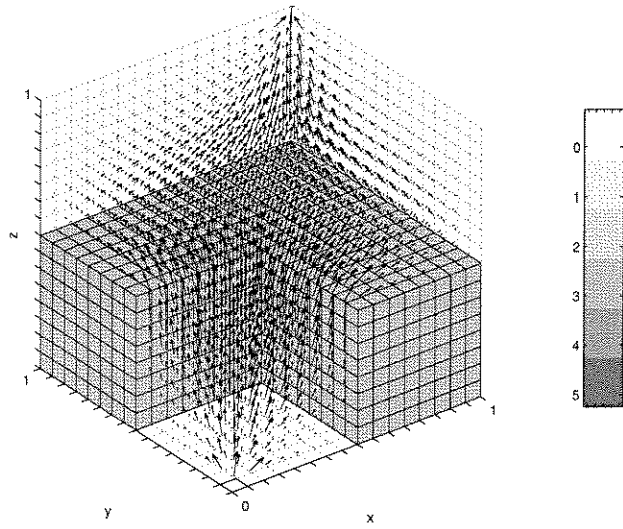
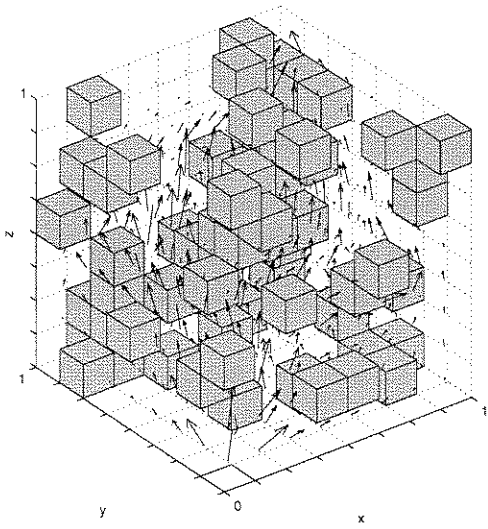
- Standard flow conceptualizations \implies block-centered logically rectangular structure (quadrilaterals, hexahedra)
- Local mass conservation
- Local discrete Darcy law (co-volumes)

Slice number 0



Slice number 0





The Discretization Methods

- Mixed Finite Element Method (MFEM)
- Control Volume MFEM (CVMFEM)
- Support Operator Method (Mimetic, SOM)
- Enhanced Cell-Centered Finite Difference Method (ECCFDM)
- Multi-Point Flux Approximation control volume method (MPFA)

It seems that the similarities between the methods are due to the following qualities:

- Local conservation
 - \sum flux over all edges = accumulation term
 - Continuous flux
- Weak continuity in the pressure
 - \implies no need for Lagrange multipliers.
- MFEM, CVMFEM, SOM: $\mathbf{K}^{-1}f = \Delta p$
- ECCFDM, MPFA: $f = \mathbf{K}\Delta p$
- Can relate via mass lumping and incomplete inversion of mass matrix

Outline

- MFEM
- Mixed Hybrid FEM, Lagrange multipliers, continuity of p
- Quadrilaterals, Piola transform
- CVMFEM
 - as MFEM
 - weak continuity of p
- SOM
 - as MFEM
 - as itself
 - weak continuity of p
- Expanded MFEM (EMFEM, basis of ECCFDM)
 - as CCFDM
 - Lack of continuity of p
- MPFA
 - as EMFEM with different test space
 - effective weak continuity of p
- A 3D example
- Approximation of solutions with singular velocities

Mixed Finite Element Methods, MFEM

$$\begin{aligned} \mathbf{u} &= -\mathbf{K}(\mathbf{x}) \operatorname{grad} p & p &\in H^1 \\ \operatorname{div} \mathbf{u} &= g & \mathbf{u} &\in H(\operatorname{div}) \end{aligned}$$

Let (\cdot, \cdot) denote the \mathcal{L}^2 -inner product

$$(\operatorname{grad} p, \mathbf{v}) = - \sum_i \int_{\partial\Omega_i} \mathbf{v} \cdot \mathbf{n} p \, ds + (\operatorname{div}_h \mathbf{v}, p)$$

Weak formulation: $(\mathbf{u}, p) \in H(\operatorname{div}) \times \mathcal{L}^2$

such that

$$\begin{aligned} (\mathbf{K}^{-1} \mathbf{u}, \mathbf{v}) - (p, \operatorname{div} \mathbf{v}) &= 0, & \text{for all } \mathbf{v} \in H(\operatorname{div}), \\ (\operatorname{div} \mathbf{u}, q) &= (g, q) & \text{for all } q \in \mathcal{L}^2, \end{aligned}$$

MFEM: $(\mathbf{u}, p) \in \mathbf{V}_h \times Q_h \subset H(\operatorname{div}) \times \mathcal{L}^2$ such that

$$\begin{aligned} a(\mathbf{u}, \mathbf{v}) - (p, \operatorname{div} \mathbf{v}) &= 0, & \mathbf{v} \in \mathbf{V}_h, \\ (\operatorname{div} \mathbf{u}, q) &= (g, q), & q \in Q_h. \end{aligned}$$

Advantages

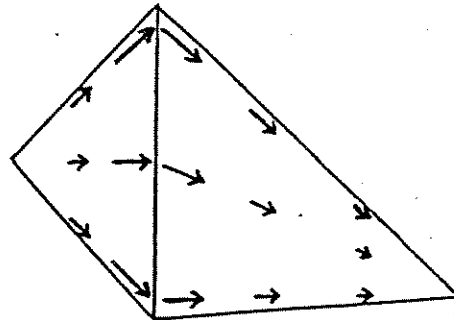
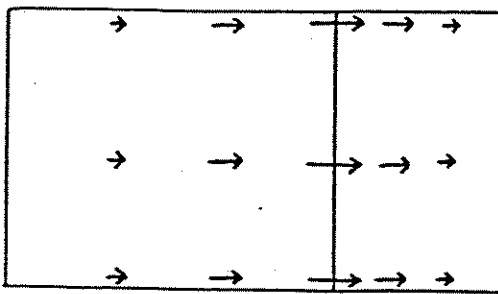
- More accurate velocity for same amount of work (heterogeneous K)
- Like block-centered finite differences (cell pressure, interblock flux, local conservation)

Disadvantages

- More algebraic equations to solve
- Equations not positive definite (bad for iterative methods)
- On irregular grids: reduced accuracy, complicated formulations

Shape and weighting functions are the same

- Velocity — associate with unit interblock flux across edge
- Velocity can be integrated analytically to give exact local and global mass conservation in FVELLAM
- Pressure — associate with unit pressure (constant) in cell



Lagrange Multipliers

Hybrid MFEM: $(\mathbf{u}, p, \lambda) \in \mathbf{V}_h^{-1} \times Q_h \times \Lambda_h$ such that

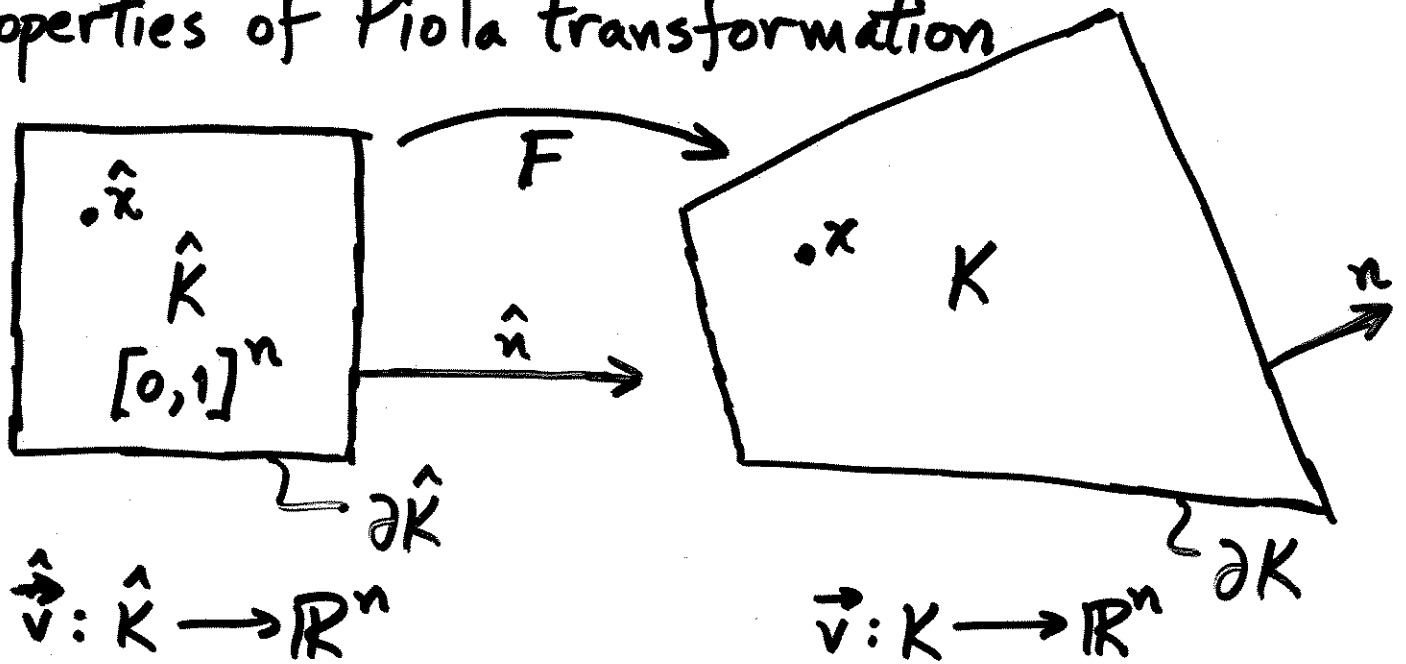
$$a(\mathbf{u}, \mathbf{v}) - (p, \operatorname{div} \mathbf{v}) + \sum_{\text{edges}} \int_e [\mathbf{v} \cdot \mathbf{n}] \lambda \, ds = 0, \quad \mathbf{v} \in \mathbf{V}_h^{-1}$$

$$(\operatorname{div} \mathbf{u}, q) = (g, q), \quad q \in Q_h$$

$$\sum_{\text{edges}} \int_e [\mathbf{u} \cdot \mathbf{n}] \mu \, ds = 0, \quad \mu \in \Lambda_h$$

PS. This does not change the solution (\mathbf{u}, p)

Properties of Piola transformation



$$\mathbf{v}(\mathbf{x}) = \frac{DF(\hat{\mathbf{x}})}{J(\hat{\mathbf{x}})} \hat{\mathbf{v}}(\hat{\mathbf{x}})$$

Preserves normal fluxes across surfaces:

$$\int_{\partial K} \mathbf{v} \cdot \mathbf{n} \, ds = \int_{\partial \hat{K}} \hat{\mathbf{v}} \cdot \hat{\mathbf{n}} \, ds \circ F$$

$\hat{\mathbf{v}} = \mathbf{RT}_0$ basis function for face $\hat{x} = 1$

$\implies \hat{\mathbf{v}}(\hat{\mathbf{x}}) = (\hat{x}, 0)$ in 2-D, $(\hat{x}, 0, 0)$ in 3-D

for \mathbf{v} { \implies flux across $\hat{x} = c$ is c (normal component = c / surface Jacobian, pointwise)
flux across $\hat{y} = c$ or $\hat{z} = c$ is 0, pointwise

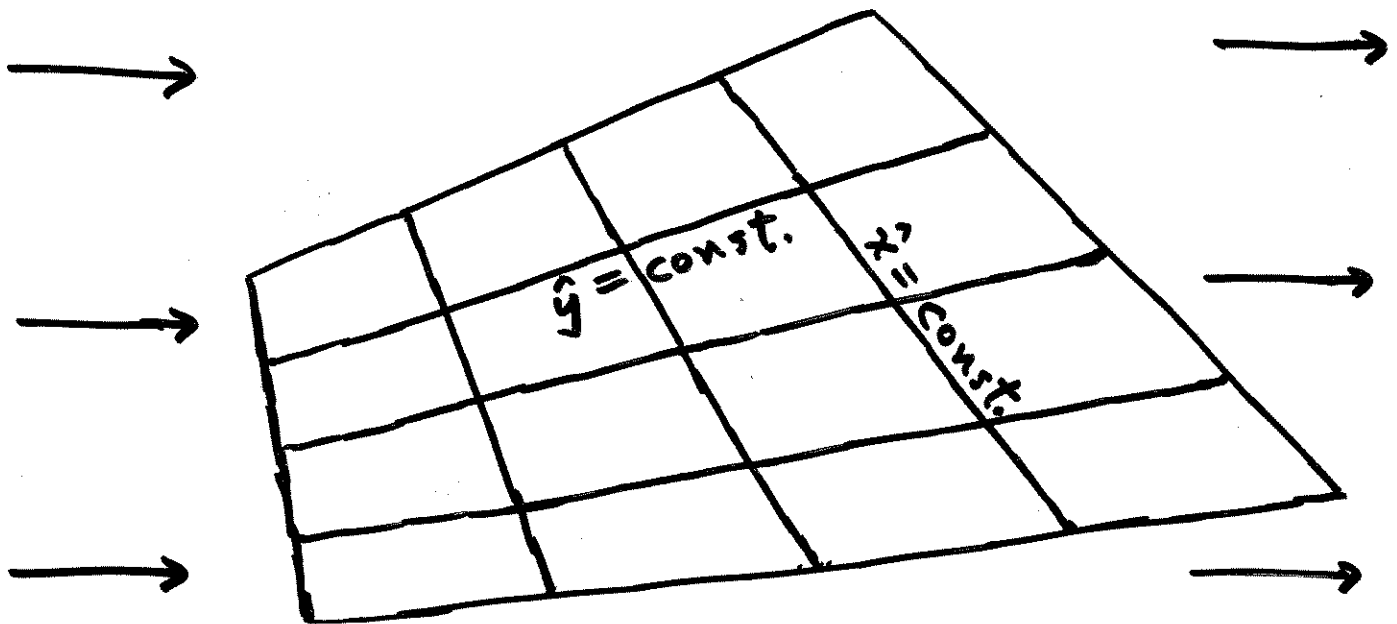
Trial space $\text{Piola}(\text{RT}_0)$ characterized by:

Normal flux across $\hat{x} = \text{const.}$ (resp. $\hat{y} = \text{const.}, \hat{z} = \text{const.}$)
is a linear function of \hat{x} (resp. \hat{y}, \hat{z})

Normal component across \hat{x} or \hat{y} or $\hat{z} = \text{const.}$
is proportional to $1/\text{surface Jacobian}$

In 2-D, constant vector field $\in \text{Piola}(\text{RT}_0)$

Note that surface (edge) Jacobian is constant



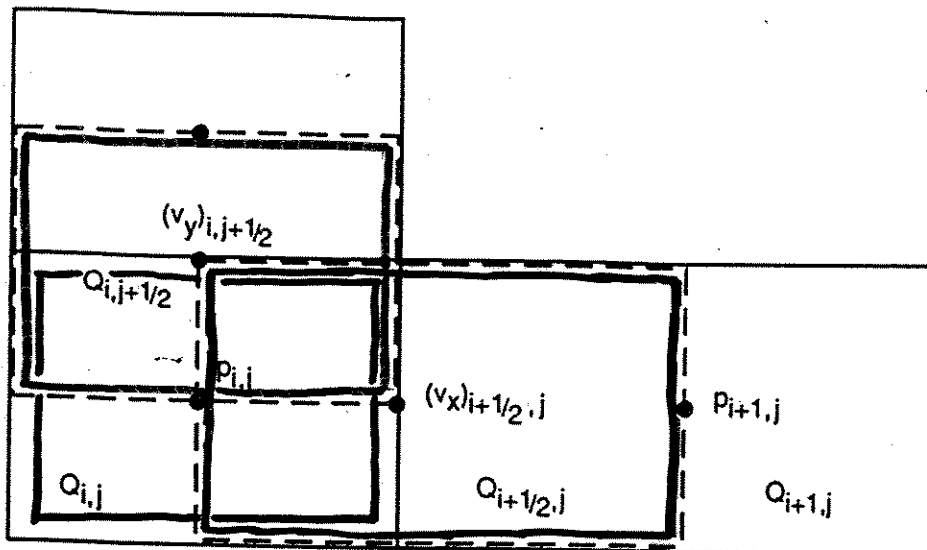
Constant vector field (in any direction)
satisfies properties above

CONTROL-VOLUME MIXED METHOD ON RECTANGLES

Shape and weighting functions are different

- Shape functions as in standard mixed method
- Velocity weighting functions constant on halves of cells
- Pressure weighting functions as in standard mixed method

$$\begin{aligned} \underline{Q}_{i,j} &= (x_{i-1/2}, x_{i+1/2}) \times (y_{j-1/2}, y_{j+1/2}), \\ \underline{Q}_{i+1/2,j} &= (x_i, x_{i+1}) \times (y_{j-1/2}, y_{j+1/2}), \\ \underline{Q}_{i,j+1/2} &= (x_{i-1/2}, x_{i+1/2}) \times (y_j, y_{j+1}), \end{aligned}$$



Discrete Darcy law:

Integrate x -component of Darcy equation over $Q_{i+1/2,j}$
(assuming rectangular grid and scalar $\Lambda = \lambda$:

$$\lambda^{-1} v_x + \frac{\partial p}{\partial x} = 0, \quad (1)$$

$$\int_{x_i}^{x_{i+1}} \int_{y_{j-1/2}}^{y_{j+1/2}} \lambda^{-1} v_x(x, y) dy dx + \int_{y_{j-1/2}}^{y_{j+1/2}} (p(x_{i+1}, y) - p(x_i, y)) dy = 0. \quad (2)$$

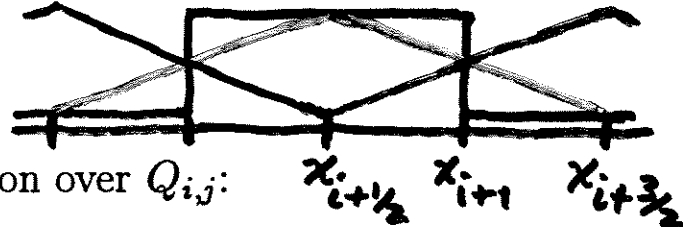
Unknown $f_x = 1$ corresponds to $v_x = 1/\Delta y$, hence

$$a_{i+1/2,j;i-1/2,j}(f_x)_{i-1/2,j} + a_{i+1/2,j;i+1/2,j}(f_x)_{i+1/2,j} + a_{i+1/2,j;i+3/2,j}(f_x)_{i+3/2,j} + p_{i+1,j} - p_{i,j} = 0,$$

where

$$\begin{aligned} \underline{a_{i+1/2,j;i-1/2,j}} &= \frac{1}{8} \frac{\lambda_{i,j}^{-1}}{|Q_{i,j}|} (x_{i+1/2} - x_{i-1/2})^2, \\ \underline{a_{i+1/2,j;i+1/2,j}} &= \frac{3}{8} \frac{\lambda_{i,j}^{-1}}{|Q_{i,j}|} (x_{i+1/2} - x_{i-1/2})^2 \\ &\quad + \frac{3}{8} \frac{\lambda_{i+1,j}^{-1}}{|Q_{i+1,j}|} (x_{i+3/2} - x_{i+1/2})^2, \\ \underline{a_{i+1/2,j;i+3/2,j}} &= \frac{1}{8} \frac{\lambda_{i+1,j}^{-1}}{|Q_{i+1,j}|} (x_{i+3/2} - x_{i+1/2})^2. \end{aligned}$$

Similarly for y -component



Integrate conservation-of-mass equation over $Q_{i,j}$:

$$\begin{aligned} (f_x)_{i-1/2,j} - (f_x)_{i+1/2,j} + (f_y)_{i,j-1/2} - (f_y)_{i,j+1/2} \\ = -|Q_{i,j}| q_{i,j}. \end{aligned}$$

Thm: (S.H. Chou, D.Y. Kwak, K.Y. Kim) Also for quadrilaterals
 $\|p - P\|_{L^2} = O(h^2)$ $\|\vec{v} - \vec{V}\|_{H(\text{div})} = O(h)$

CONTROL-VOLUME MIXED METHOD ON QUADRILATERALS

Reference mapping

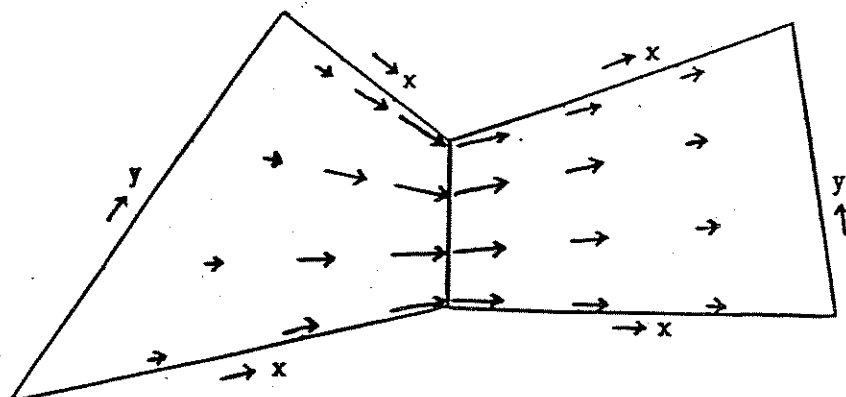
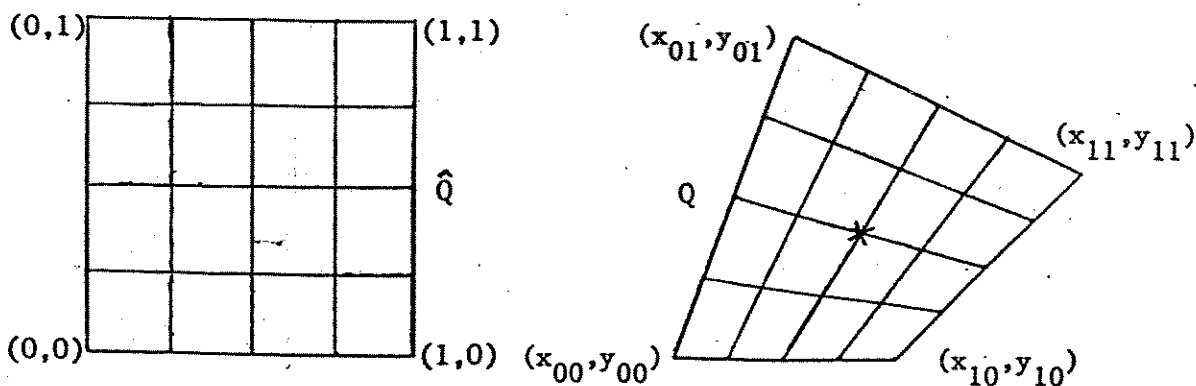
$$\begin{aligned}
 x(\hat{x}, \hat{y}) &= x_{00} + (x_{10} - x_{00})\hat{x} + (x_{01} - x_{00})\hat{y} \\
 &\quad + (x_{11} - x_{10} - x_{01} + x_{00})\hat{x}\hat{y}, \\
 y(\hat{x}, \hat{y}) &= y_{00} + (y_{10} - y_{00})\hat{x} + (y_{01} - y_{00})\hat{y} \\
 &\quad + (y_{11} - y_{10} - y_{01} + y_{00})\hat{x}\hat{y}.
 \end{aligned}$$

Inverse mapping exists for convex quadrilaterals

Pressure shape functions: constant on cells $Q_{i,j}$

Velocity shape functions:

- Correspond to unit flux across each edge
- Constant normal component on edge, continuous

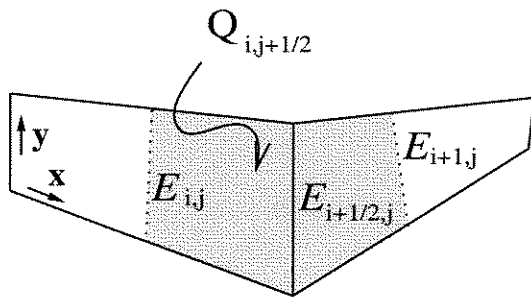


CVMFEM as MFEM

$(\mathbf{u}, p) \in \mathbf{V}_h \times Q_h$ such that

$$\begin{aligned} a(\mathbf{u}, \gamma_h \mathbf{v}) + (p, \operatorname{div}_h \gamma_h \mathbf{v}) &= 0, & \mathbf{v} \in \mathbf{V}_h, \\ (\operatorname{div} \mathbf{u}, q) &= (g, q), & q \in Q_h. \end{aligned}$$

- $\operatorname{supp}(\gamma_h \mathbf{v}_{i,j+1/2}) = Q_{i,j+1/2}$
- $\gamma_h : \mathbf{V}_h \rightarrow \mathbf{Y}_h$
- $\gamma_h \mathbf{v}$, chosen such that $\int_r [p] ds = 0$



Garanza and Konshin type Test Function
Applied to Pressure Gradient

Computer Centre
Russian Acad. Sc
Moscow, 1999
2-D

$$\begin{aligned}
 & \int_{Q_{i+1/2,j,k}} \nabla p \cdot \frac{\vec{X}}{J} dx dy dz \\
 &= \int_{Q_{i+1/4,j,k}} \frac{\nabla p \cdot \vec{X}_{i,j,k}}{J_{i,j,k}} dx dy dz + \int_{Q_{i+3/4,j,k}} \frac{\nabla p \cdot \vec{X}_{i+1,j,k}}{J_{i+1,j,k}} dx dy dz \\
 &= \int_0^1 \int_0^1 \int_{1/2}^1 \nabla p \cdot \vec{X}_{i,j,k} d\hat{x} d\hat{y} d\hat{z} + \int_0^1 \int_0^1 \int_0^{1/2} \nabla p \cdot \vec{X}_{i+1,j,k} d\hat{x} d\hat{y} d\hat{z} \\
 &= \int_0^1 \int_0^1 \int_{1/2}^1 \frac{\partial p}{\partial \hat{x}} \Big|_{Q_{i+1/4,j,k}} d\hat{x} d\hat{y} d\hat{z} + \int_0^1 \int_0^1 \int_0^{1/2} \frac{\partial p}{\partial \hat{x}} \Big|_{Q_{i+3/4,j,k}} d\hat{x} d\hat{y} d\hat{z} \\
 &= \int_0^1 \int_0^1 (p|_{\hat{x}=1} - p|_{\hat{x}=1/2}) \Big|_{Q_{i+1/4,j,k}} d\hat{y} d\hat{z} + \int_0^1 \int_0^1 (p|_{\hat{x}=1/2} - p|_{\hat{x}=0}) \Big|_{Q_{i+3/4,j,k}} d\hat{y} d\hat{z} \\
 &= \int_0^1 \int_0^1 p|_{\hat{x}=1/2} d\hat{y} d\hat{z} \Big|_{Q_{i+3/4,j,k}} - \int_0^1 \int_0^1 p|_{\hat{x}=1/2} d\hat{y} d\hat{z} \Big|_{Q_{i+1/4,j,k}} \\
 &\approx p_{i+1,j,k} - p_{i,j,k}
 \end{aligned}$$

$$\vec{w}_{i+1/2,j,k} = \begin{cases} \vec{X}_{i,j,k} / J_{i,j,k}(\hat{x}, \hat{y}, \hat{z}), & \text{on } Q_{i+1/4,j,k} \\ \vec{X}_{i+1,j,k} / J_{i+1,j,k}(\hat{x}, \hat{y}, \hat{z}), & \text{on } Q_{i+3/4,j,k} \\ 0, & \text{otherwise} \end{cases}$$

Conservation-of-mass equation (same form as on rectangles):

$$(f_x)_{i-1/2,j} - (f_x)_{i+1/2,j} + (f_y)_{i,j-1/2} - (f_y)_{i,j+1/2} = -|Q_{i,j}|q_{i,j}.$$

Darcy equation and coefficients:

$$\begin{aligned} a_{i+1/2,j;i-1/2,j}(f_x)_{i-1/2,j} + a_{i+1/2,j;i+1/2,j}(f_x)_{i+1/2,j} \\ + a_{i+1/2,j;i+3/2,j}(f_x)_{i+3/2,j} \\ + a_{i+1/2,j;i,j+1/2}(f_y)_{i,j+1/2} + a_{i+1/2,j;i,j-1/2}(f_y)_{i,j-1/2} \\ + a_{i+1/2,j;i+1,j+1/2}(f_y)_{i+1,j+1/2} + a_{i+1/2,j;i+1,j-1/2}(f_y)_{i+1,j-1/2} \\ + p_{i+1,j} - p_{i,j} = 0, \end{aligned}$$

$$\begin{aligned} a_{i+1/2,j;i+1/2,j} = \int_0^1 \int_{1/2}^1 \frac{\hat{x}}{J_{i,j}(\hat{x}, \hat{y})} (\mathbf{K}_{i,j}^{-1} \mathbf{X}) \cdot \mathbf{X} d\hat{x} d\hat{y} \\ + \int_0^1 \int_0^{1/2} \frac{1 - \hat{x}}{J_{i+1,j}(\hat{x}, \hat{y})} (\mathbf{K}_{i+1,j}^{-1} \mathbf{X}) \cdot \mathbf{X} d\hat{x} d\hat{y}, \end{aligned}$$

$$a_{i+1/2,j;i-1/2,j} = \int_0^1 \int_{1/2}^1 \frac{1 - \hat{x}}{J_{i,j}(\hat{x}, \hat{y})} (\mathbf{K}_{i,j}^{-1} \mathbf{X}) \cdot \mathbf{X} d\hat{x} d\hat{y},$$

$$a_{i+1/2,j;i+3/2,j} = \int_0^1 \int_0^{1/2} \frac{\hat{x}}{J_{i+1,j}(\hat{x}, \hat{y})} (\mathbf{K}_{i+1,j}^{-1} \mathbf{X}) \cdot \mathbf{X} d\hat{x} d\hat{y},$$

$$a_{i+1/2,j;i,j+1/2} = \int_0^1 \int_{1/2}^1 \frac{\hat{y}}{J_{i,j}(\hat{x}, \hat{y})} (\mathbf{K}_{i,j}^{-1} \mathbf{Y}) \cdot \mathbf{X} d\hat{x} d\hat{y},$$

$$a_{i+1/2,j;i,j-1/2} = \int_0^1 \int_{1/2}^1 \frac{1 - \hat{y}}{J_{i,j}(\hat{x}, \hat{y})} (\mathbf{K}_{i,j}^{-1} \mathbf{Y}) \cdot \mathbf{X} d\hat{x} d\hat{y},$$

$$a_{i+1/2,j;i+1,j+1/2} = \int_0^1 \int_0^{1/2} \frac{\hat{y}}{J_{i+1,j}(\hat{x}, \hat{y})} (\mathbf{K}_{i+1,j}^{-1} \mathbf{Y}) \cdot \mathbf{X} d\hat{x} d\hat{y},$$

$$a_{i+1/2,j;i+1,j-1/2} = \int_0^1 \int_0^{1/2} \frac{1 - \hat{y}}{J_{i+1,j}(\hat{x}, \hat{y})} (\mathbf{K}_{i+1,j}^{-1} \mathbf{Y}) \cdot \mathbf{X} d\hat{x} d\hat{y}.$$

SOM in Framework of MFEM

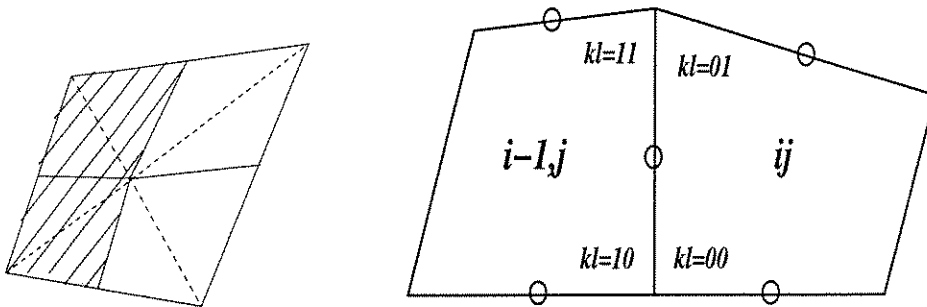
$$\begin{aligned} \mathbf{u} &= \mathcal{G} p \\ \mathcal{D} \mathbf{u} &= G. \end{aligned}$$

For $\mathcal{G} = \mathcal{S}^{-1} \mathcal{D}' \mathcal{M}$

$$\begin{aligned} \mathcal{S} \mathbf{u} &= \mathcal{D}' \mathcal{M} p, \\ \mathcal{D} \mathbf{u} &= G. \end{aligned}$$

From MFEM with \mathbf{RT}_0 elements, and

$$a_{h,S}(\mathbf{u}, \mathbf{v})|_K = \mathcal{S} \mathbf{u}|_K = \sum_{i=0}^4 A_i(\mathbf{u}^T \mathbf{K}^{-1} \mathbf{v})$$



The Original Outline of SOM

Define a natural inner product

$$(p, q)_{\text{HC}} = \sum_{\text{elements}} A_{ij} p_{ij} q_{ij}$$

$$(\mathbf{A}, \mathbf{B})_{\text{HS}} = \sum_{\text{elements}} A_{ij} (\mathbf{A}, \mathbf{B})_{ij}$$

$$\text{- for } (\mathbf{A}, \mathbf{B})_{ij} = \sum_{\text{vertex}} A_v (\mathbf{G}_v \mathbf{A}, \mathbf{G}_v \mathbf{B})_{ij}$$

- \mathbf{G} maps \mathbf{A} to $(A\xi, A\eta)^T$, an orthogonal grid,

$$\text{- } \mathbf{G}_v = \begin{pmatrix} 1 & 0 \\ -\cos(\phi_v) & \sin(\phi_v) \end{pmatrix}.$$

And a formal inner product

$$[p, q]_{\text{HC}} = \sum_{\text{elements}} p_{ij} q_{ij}$$

$$[\mathbf{A}, \mathbf{B}]_{\text{HS}} = \sum_{\text{'x'-edges}} A\xi_e B\xi_e + \sum_{\text{'y'-edges}} A\eta_e B\eta_e$$

The main assumption.

$$(\mathcal{D}\mathbf{u}, p)_{\text{HC}} = (\mathbf{u}, \mathcal{D}^*p)_{\text{HS}}$$

$\mathcal{D}^* = \mathcal{G}$ = approximation of $-\mathbf{K}$ grad

Equivalent to

$$(\mathcal{D}\mathbf{u}, p)_{\text{num.int}} = (\mathbf{u}, \mathcal{D}^*p)_{\text{num.int}}$$

An approximation to

$$\int_{\Omega} \mathcal{D}\mathbf{u} p \, d\mathbf{x} = \int_{\Omega} \mathbf{u}^T \mathcal{D}^*p \, d\mathbf{x}$$

In the framework of MHFEM, the Lagrange multiplier term is zero, i.e., the SOM imposes a weak continuity of p .

The Expanded MFEM

$$\begin{aligned}\mathbf{u} &= \mathbf{K}(\mathbf{x})\tilde{\mathbf{u}} \\ \tilde{\mathbf{u}} &= -\text{grad } p, \\ \text{div } \mathbf{u} &= g.\end{aligned}$$

Find $(\mathbf{u}, \tilde{\mathbf{u}}, p) \in \mathbf{V}_h \times \tilde{\mathbf{V}}_h \times Q_h \subset H(\text{div}) \times (\mathcal{L}^2)^2 \times \mathcal{L}^2$ such that

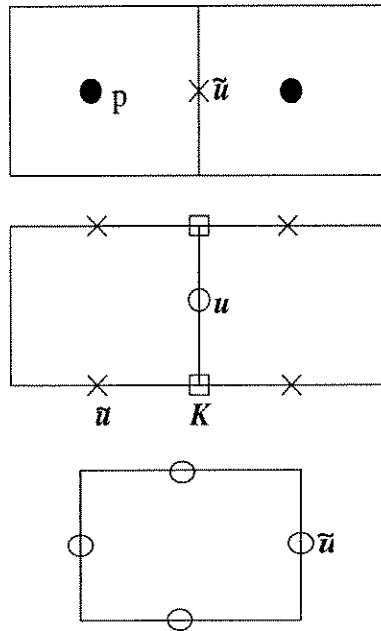
$$\begin{aligned}(\tilde{\mathbf{u}}, \mathbf{v}) - (p, \text{div } \mathbf{v}) &= 0, & \text{for all } \mathbf{v} \in \mathbf{V}_h, \\ (\mathbf{u}, \tilde{\mathbf{v}}) - (\mathbf{K}\tilde{\mathbf{u}}, \tilde{\mathbf{v}}) &= 0, & \text{for all } \tilde{\mathbf{v}} \in \tilde{\mathbf{V}}_h, \\ (\text{div } \mathbf{u}, q) &= (g, q), & \text{for all } q \in Q_h.\end{aligned}$$

$$\mathbf{V}_h = \mathbf{RT}_0, \quad \tilde{\mathbf{V}}_h = ?, \quad Q_h = \mathbb{P}_0^{-1}$$

$\tilde{\mathbf{V}}_h = \text{rectangular/quadrilateral Hodge }^* \text{ of } \mathbf{RT}_0?$

Enhanced Cell-Centered Finite Difference Method

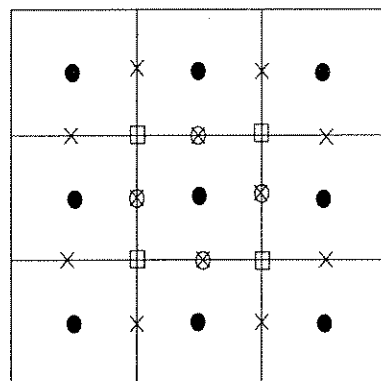
$$V_h = \tilde{V}_h = \mathbf{RT}_0 + \text{num.int}$$



In the reference space $\mathcal{K} = \mathbf{J} \mathbf{D}\mathbf{F}^{-1} \mathbf{K} \mathbf{D}\mathbf{F}^{-1}$,

\mathbf{J} = Jacobian

$\mathbf{D}\mathbf{F}$ = Jacobian matrix



Discontinuous Permeability

Orthogonal grids with diagonal permeability
 \implies 1D case in each direction

1D & cell-centered FDM:

Harmonic mean of the permeability maintains the order of convergence, while arithmetic mean reduces it.

(ref: A.A. Samarskij)

Harmonic mean:

$$f = -\frac{2}{\frac{h_i}{k_i} + \frac{h_{i+1}}{k_{i+1}}}(p_{i+1} - p_i)$$

Found from the assumption of

- continuous velocity
- continuous pressure

Rectangular grids & discontinuous orthogonal permeability

- MFEM and RT_0 elements*
- CVMFEM*
- SOM
- MPFA**

Reduces to FDM with harmonic mean

* with trapezoidal integration rule

** on \mathbf{K} -orthogonal grid

- Cell-Centered FDM derived from EMFEM

$$\mathbf{u}_{i+1/2,j}^x = -\frac{h_i k_i + h_{i+1} k_{i+1}}{1/2(h_i + h_{i+1})^2} (p_{i+1} - p_i)$$

Numerical examples show that the order of convergence is reduced

The order of convergence can be maintained if Lagrange multipliers are added along the discontinuity (ECCFDM)
 \implies enforce a weak continuity of the pressure.

Observation:

Weak continuity in the pressure is related to the rate of convergence across a discontinuity in the media.
--

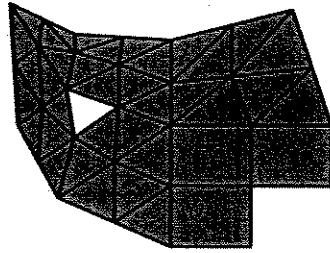


FIG. 10.3. A complex domain with a hierarchical mesh.

TABLE 10.1

The pressure error $\|P - p\|_M$ and the velocity error $\|U - u\|_M$ for a hierarchical example.

h	Mixed		Unenhanced cell-centered		Enhanced cell-centered	
	p	u	p	u	p	u
0.16	0.39	6.0	0.48	9.3	0.59	6.4
0.08	0.11	3.1	0.12	5.9	0.11	3.5
0.04	0.029	1.5	0.043	3.7	0.026	1.6
0.02	0.0076	0.77	0.019	2.5	0.0062	0.80
Rate	h^2	h	$h^{1.4}$	$h^{0.6}$	h^2	h

Different Approximation Spaces

Needed if $\mathbf{u} = \mathbf{K}\tilde{\mathbf{u}}$, and \mathbf{u} has continuous normal component, while \mathbf{K} is discontinuous.

Find $(\mathbf{u}, \tilde{\mathbf{u}}, p) \in \mathbf{RT}_0 \times \mathbf{RT}_0^{-1} \times Q_h$ such that

$$\begin{aligned}(\tilde{\mathbf{u}}, \mathbf{v}) - (p, \operatorname{div} \mathbf{v}) &= 0, & \text{for all } \mathbf{v} \in \mathbf{RT}_0, \\(\mathbf{u}, \tilde{\mathbf{v}}) - (\mathbf{K}\tilde{\mathbf{u}}, \tilde{\mathbf{v}}) &= 0, & \text{for all } \tilde{\mathbf{v}} \in \mathbf{RT}_0^{-1}, \\(\operatorname{div} \mathbf{u}, q) &= (g, q), & \text{for all } q \in Q_h.\end{aligned}$$

The same numerical integration will now give the harmonic mean on an orthogonal grid with diagonal \mathbf{K} .

What about an arbitrary elementwise constant tensor \mathbf{K} ? Can't eliminate $\tilde{\mathbf{u}}$ to get a FD expression in \mathbf{u} and p .

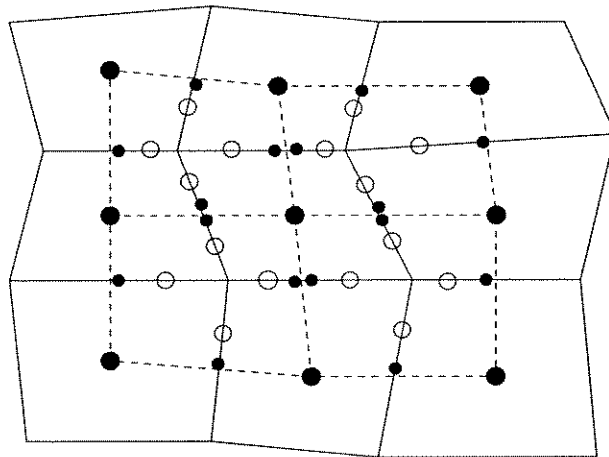
On orthogonal grid, can split flux equation for each edge into two equal half-edge parts, split edge unknowns \mathbf{u} and $\tilde{\mathbf{u}}$ each into two half-edge unknowns, then eliminate $\tilde{\mathbf{u}}$ for the four half-edges meeting at a cell vertex.

The Multi-Point Flux Approximation Control Volume Method

$$\sum_{i \in T} f_i = Q_T$$

$$f_i^{1/2} = \sum_{k=1}^4 t_k p_k$$

- Cell-centered pressure values
- Continuous flux
- Linear pressure, one point of continuity at each half edge



- The MPFA “weak continuity” of p is not equivalent to Lagrange multipliers (edge point at end of sub-edge)

Relationship between Expanded MFEM and MPFA (orthogonal grid, full-tensor \mathbf{K})

Trapezoidal numerical integration

\implies cannot eliminate $\tilde{\mathbf{u}}_{i+1/2}$ easily
($\tilde{\mathbf{u}} = \mathbf{K}\mathbf{u}$ complicated if \mathbf{K} tensor)

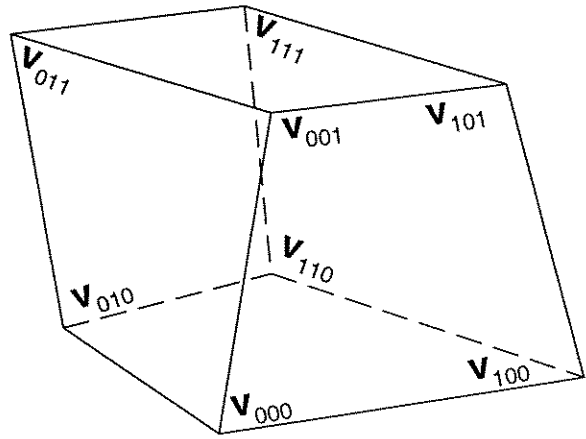
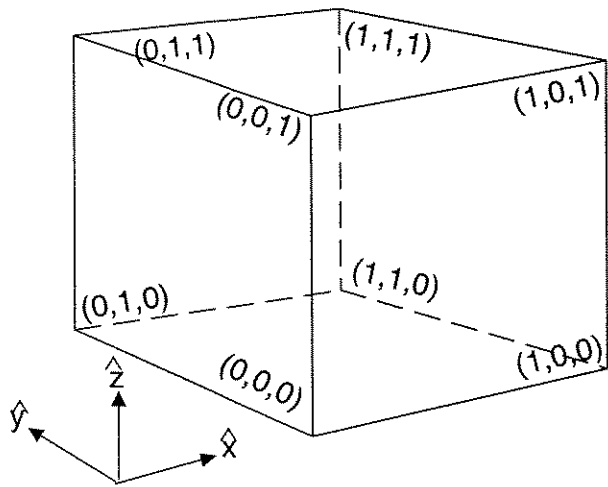
Can eliminate $\tilde{\mathbf{u}}_{i+1/2}$ by separate integration over upper and lower “interaction regions”

\implies 2 equations for each edge, amalgamation of solution of larger system solves EMFEM eqs.

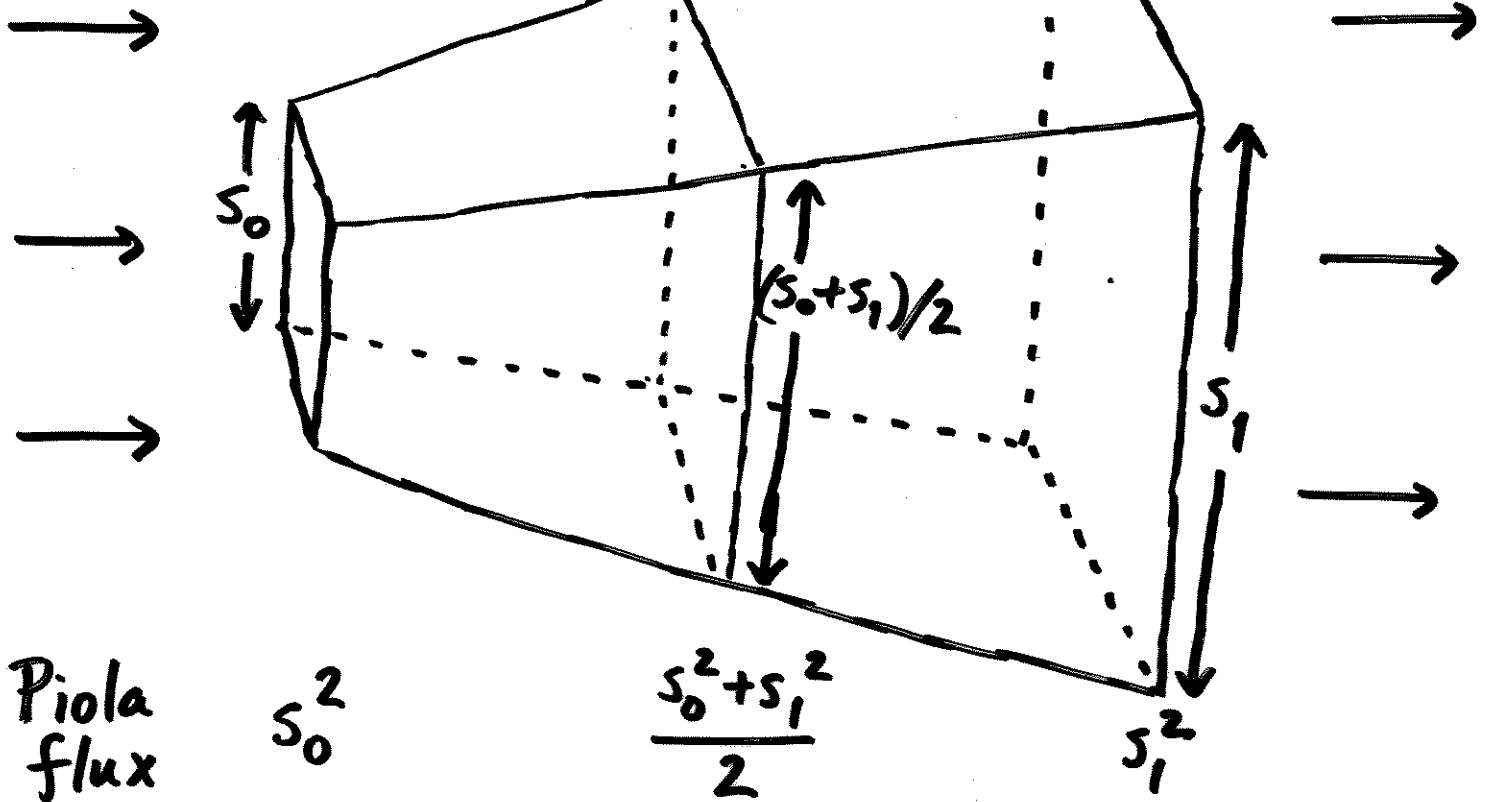
Larger system yields the MPFA “O-method” augmented by a discrete-gradient $\tilde{\mathbf{u}}$ -like variable

Amalgamated MPFA has same weak continuity of p as EMFEM with different test spaces

EMFEM error analysis can be used to prove convergence of MPFA



In 3-D, constant vector field \neq Piola (RT_0)
 Truncated pyramid

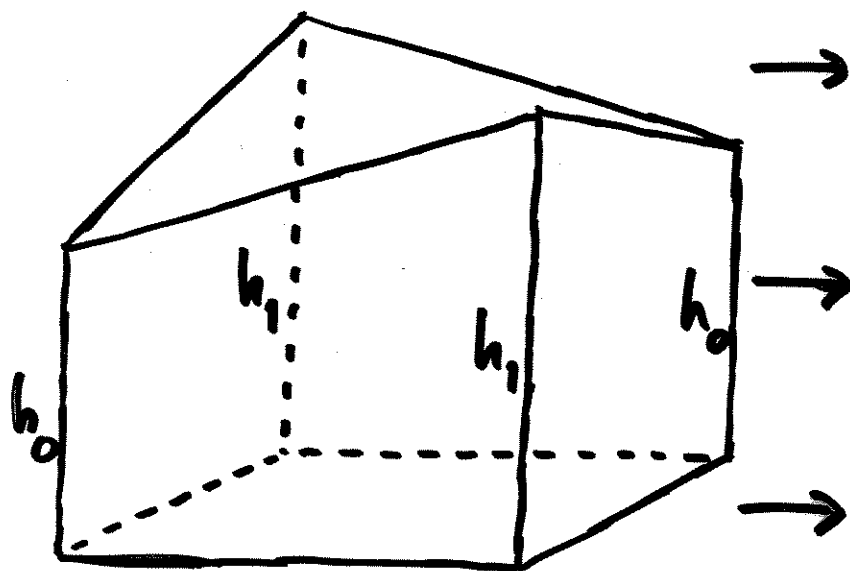


Unlike 2-D, cross-sectional area (length for 2-D) is not a linear function of \hat{x}

A further thought experiment...

Top face is $\hat{z}=1$
(curvilinear)

Net flux across
top face = 0
(not pointwise)



Basis vector fields for other 5 faces have
normal component 0 on top face, pointwise

Coefficient of basis vector field for top face is 0

\Rightarrow Trial function attempting to represent constant
vector field has 0 normal component on
top face, pointwise

Conclusion: A trial space with

(1) degrees of freedom \leftrightarrow face fluxes

(2) pointwise preservation of 0 fluxes
across surfaces

cannot (in general) contain the constant vector fields.

FLUX APPROXIMATIONS

Exact flux

$$F_x(\hat{x}) = \int_0^1 \int_0^1 V(\hat{x}, \hat{y}, \hat{z}) \cdot (Y \times Z)(\hat{x}, \hat{y}, \hat{z}) d\hat{y} d\hat{z}$$

Surface Jacobian

$$Y \times Z = (1-\hat{x}) Y_0 \times Z_0 + \hat{x} Y_1 \times Z_1 - \hat{x}(1-\hat{x}) \underbrace{(Y_1 - Y_0)}_{\delta Y} \times \underbrace{(Z_1 - Z_0)}_{\delta Z}$$

Piola approximate flux (linear interpolation)

$$LF_x(\hat{x}) = (1-\hat{x}) F_x(0) + \hat{x} F_x(1)$$

Quadratic approximate flux

$$QF_x(\hat{x}) = (1-\hat{x}) F_x(0) + \hat{x} F_x(1) - \hat{x}(1-\hat{x}) F_{xi}$$

$$F_{xi} = \int_0^1 \int_0^1 V\left(\frac{1}{2}, \hat{y}, \hat{z}\right) \cdot (\delta Y \times \delta Z) d\hat{y} d\hat{z}$$

Uniform flow (V constant) $\implies F_x \equiv QF_x$

Not necessarily exact pointwise velocities

FLUX TRUNCATION ERRORS

$$F_x - QF_x = \int_0^{\overbrace{\Delta x}^{O(\Delta x)}} \overbrace{G(x, \xi)}^{O(\Delta x)} \int_0^1 \int_0^1 \left\{ O(1) + \right.$$

$$\left. + \frac{2}{\Delta x} \frac{\partial V}{\partial x} \cdot (Y_1 \times Z_1 - Y_0 \times Z_0) \right.$$

$O(\Delta x)$ if regular refinement
 $O(1)$ if random refinement

$$\left. + \left[\frac{2}{\Delta x^2} \left(V(\xi) - \overset{\text{if } LF_x}{V\left(\frac{\Delta x}{2}\right)} \right) + O\left(\frac{1}{\Delta x}\right) \right] \cdot \right.$$

$O(1/\Delta x)$ if QF_x

$O(1/\Delta x^2)$ if LF_x

$$\cdot \left[\delta Y \times \delta Z \right] \} d\hat{y} d\hat{z} d\xi$$

$O(\Delta x^2)$ if regular

$O(1)$ if random

	$F_x - LF_x$	$F_x - QF_x$
Regular refinement	$O(\Delta x^2)$	$O(\Delta x^2)$
Random refinement	$O(1)$	$O(\Delta x)$
Uniform flow	not exact	exact

DETERMINATION OF QUADRATIC CORRECTION

Algorithm gives primary face fluxes

$$F_x(0), F_x(1), F_y(0), F_y(1), F_z(0), F_z(1)$$

(RT_0 degrees of freedom)

F_{xi} approximation, $O(\Delta x^2(\Delta x^2 + \Delta y^2 + \Delta z^2))$:

$$F_{xi} \approx \frac{1}{8} \left(\sum_{8 \text{ corners}} V(\text{corner}) \right) \cdot \int_0^1 \int_0^1 \delta Y \times \delta Z \, d\hat{y} d\hat{z}$$

($V(\text{corner})$ determined from primary face fluxes)

FROM FLUXES TO VELOCITIES (trial functions)

Normal component magnitude

$$U_x = (1 - \hat{x}) \frac{F_x(0)}{A_x(0)} \frac{|Y_0 \times Z_0|}{|Y \times Z|} + \hat{x} \frac{F_x(1)}{A_x(1)} \frac{|Y_1 \times Z_1|}{|Y \times Z|}$$

cross-sectional area $\int_0^1 \int_0^1 |Y \times Z|(\hat{x}, \hat{y}, \hat{z}) d\hat{y} d\hat{z}$

$$- \hat{x}(1 - \hat{x}) \frac{F_{xi}}{A_{xi}} \frac{|\delta Y \times \delta Z|}{|Y \times Z|}$$

$\int_0^1 \int_0^1 |\delta Y \times \delta Z|(\hat{y}, \hat{z}) d\hat{y} d\hat{z}$

Quadratic flux

$$\int_0^1 \int_0^1 U_x(\hat{x}, \hat{y}, \hat{z}) |Y \times Z| d\hat{y} d\hat{z} = Q F_x(\hat{x})$$

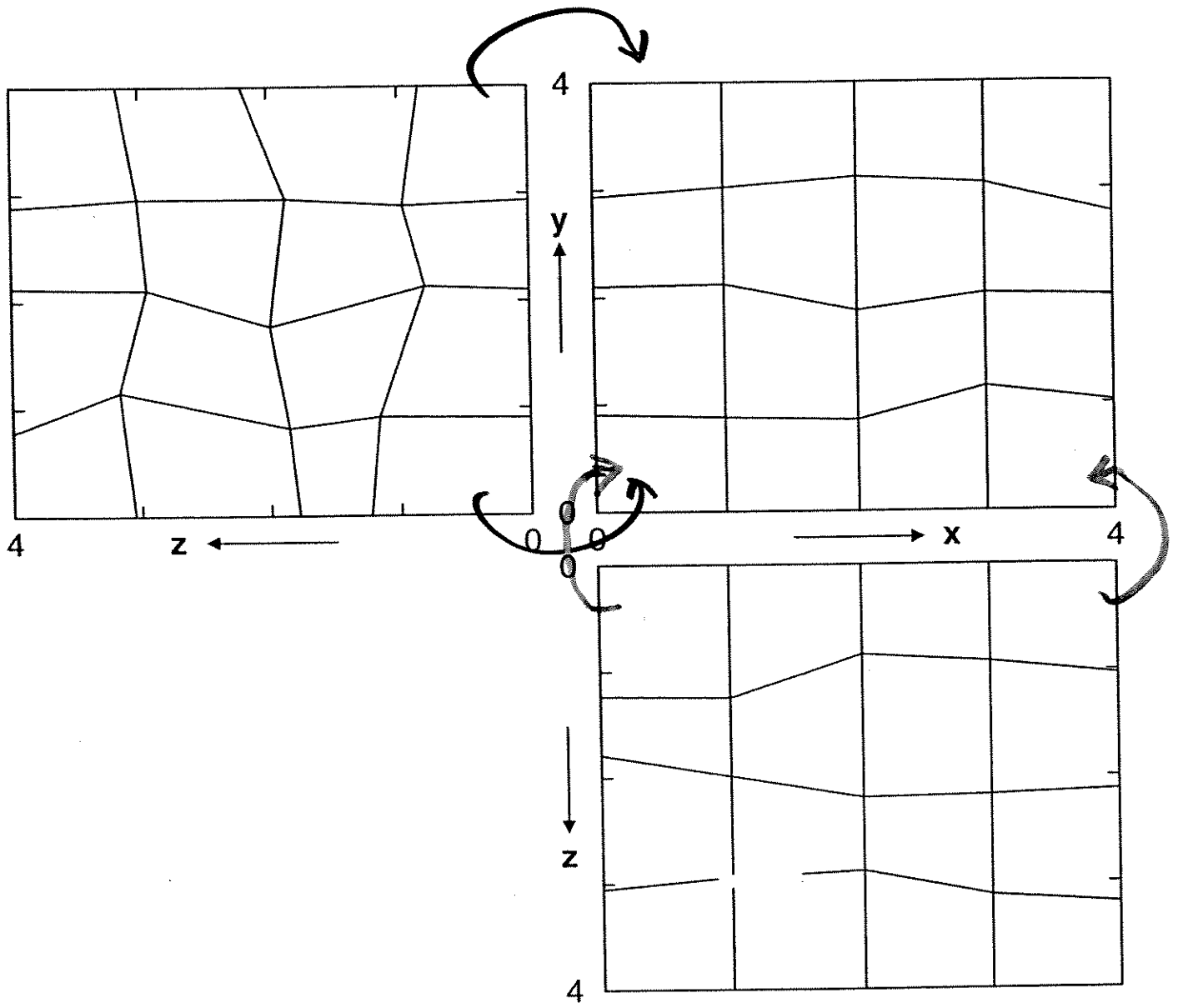
Constant normal component on primary cell faces

Velocity vector field

$$V = V_x + V_y + V_z$$

$$V_x = U_x \frac{|Y \times Z|}{J} X$$

Good for truncated pyramid (planar faces),
not for test with curved roof (non-planar)



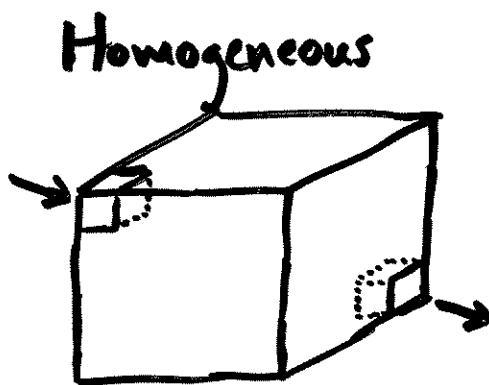
RESULTS

Uniform Flow

Grid	Planar, quasi-random faces	x-faces parallel, y-, z- quasi-random
4^3	$6.10 E-6$	exact
8^3	$2.42 E-6$	$5.83 E-5$
16^3	$7.64 E-7$	$1.27 E-5$
32^3	$2.25 E-7$	$3.90 E-6$

Non-uniform Flow

Grid	Homogeneous	Exclude 1-cell buffer around corners from error	Heterogeneous (3 orders of magnitude), mean flow in x-direction
5^3	$1.50 E-3$	$1.11 E-3$	$2.37 E-2$
10^3	$6.59 E-4$	$2.41 E-4$	$1.42 E-2$
20^3	$3.44 E-4$	$4.64 E-5$	$6.92 E-3$
40^3	Used as "exact" solution		



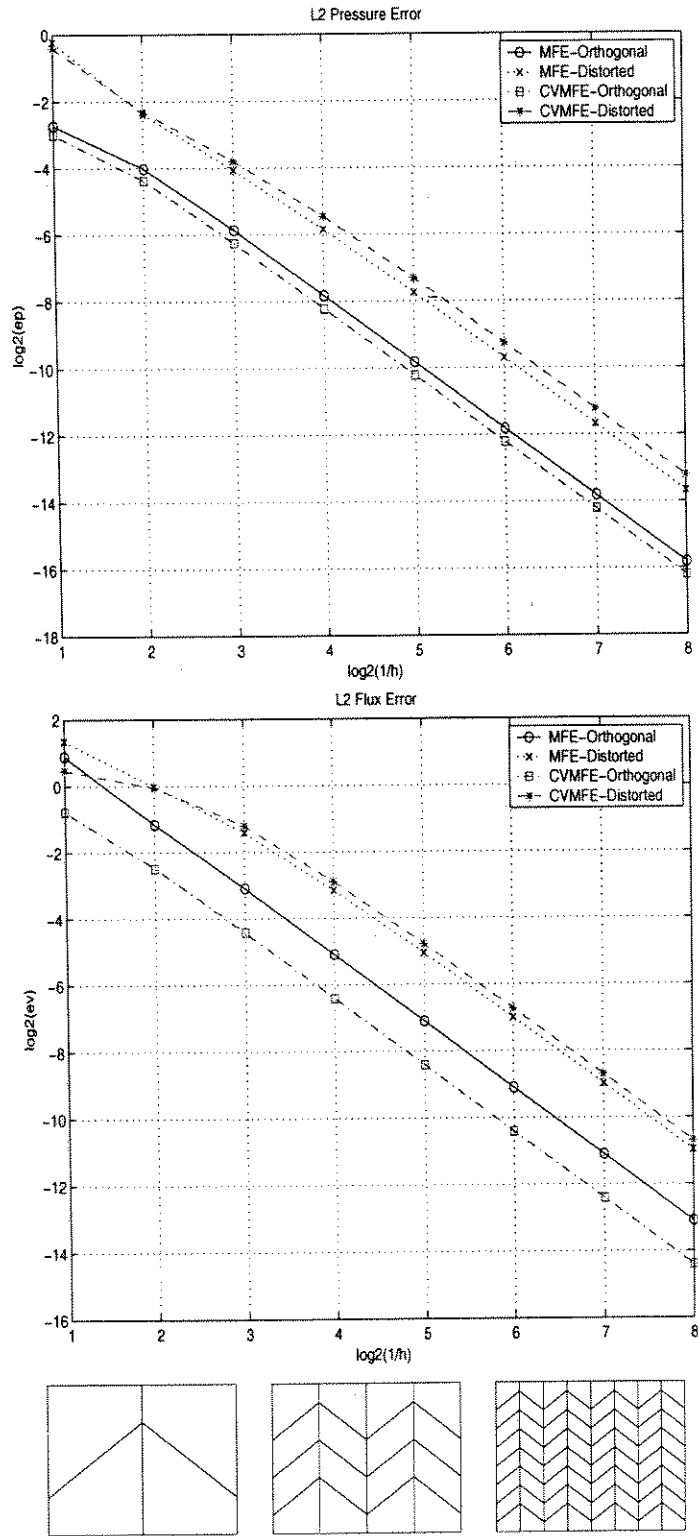
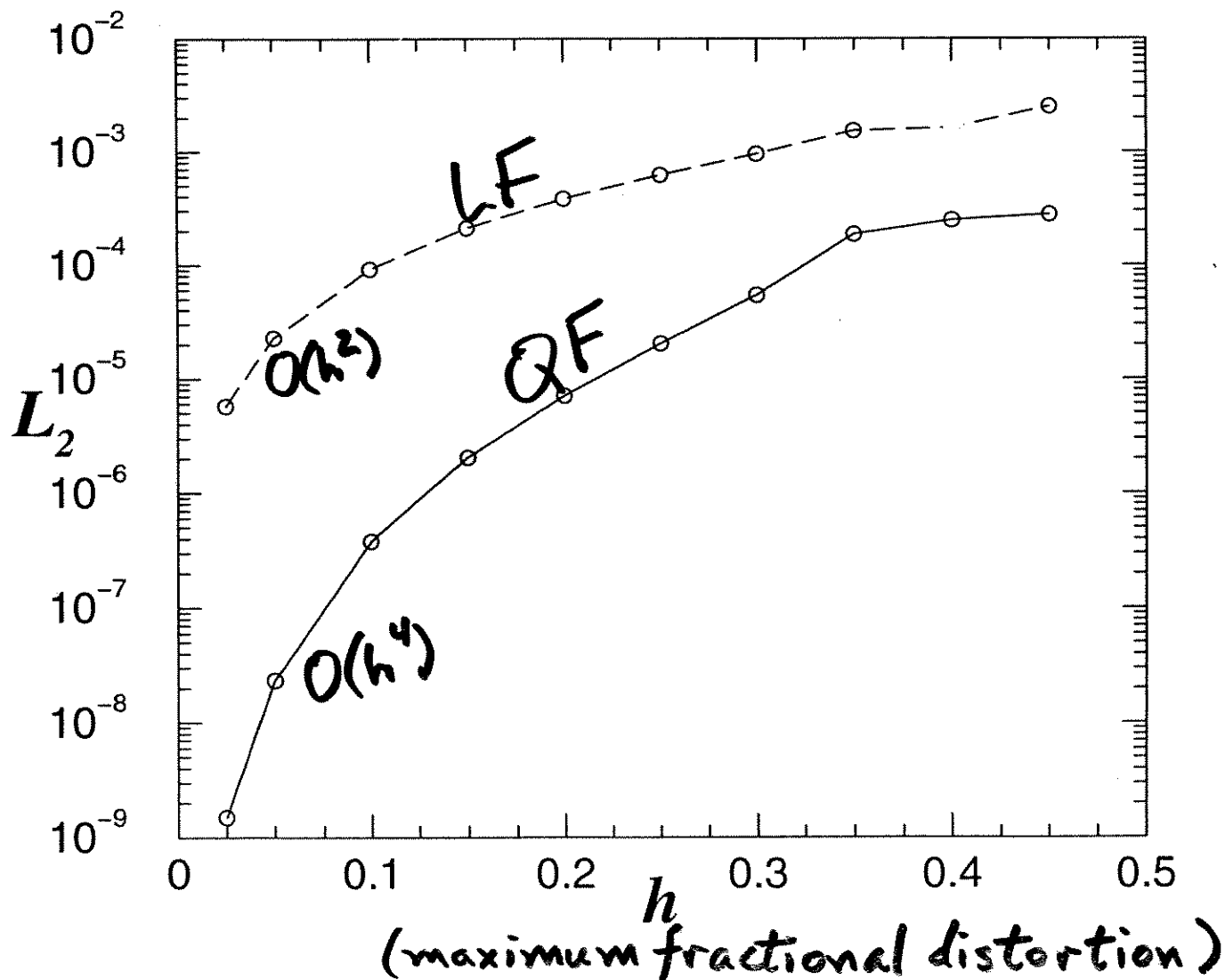
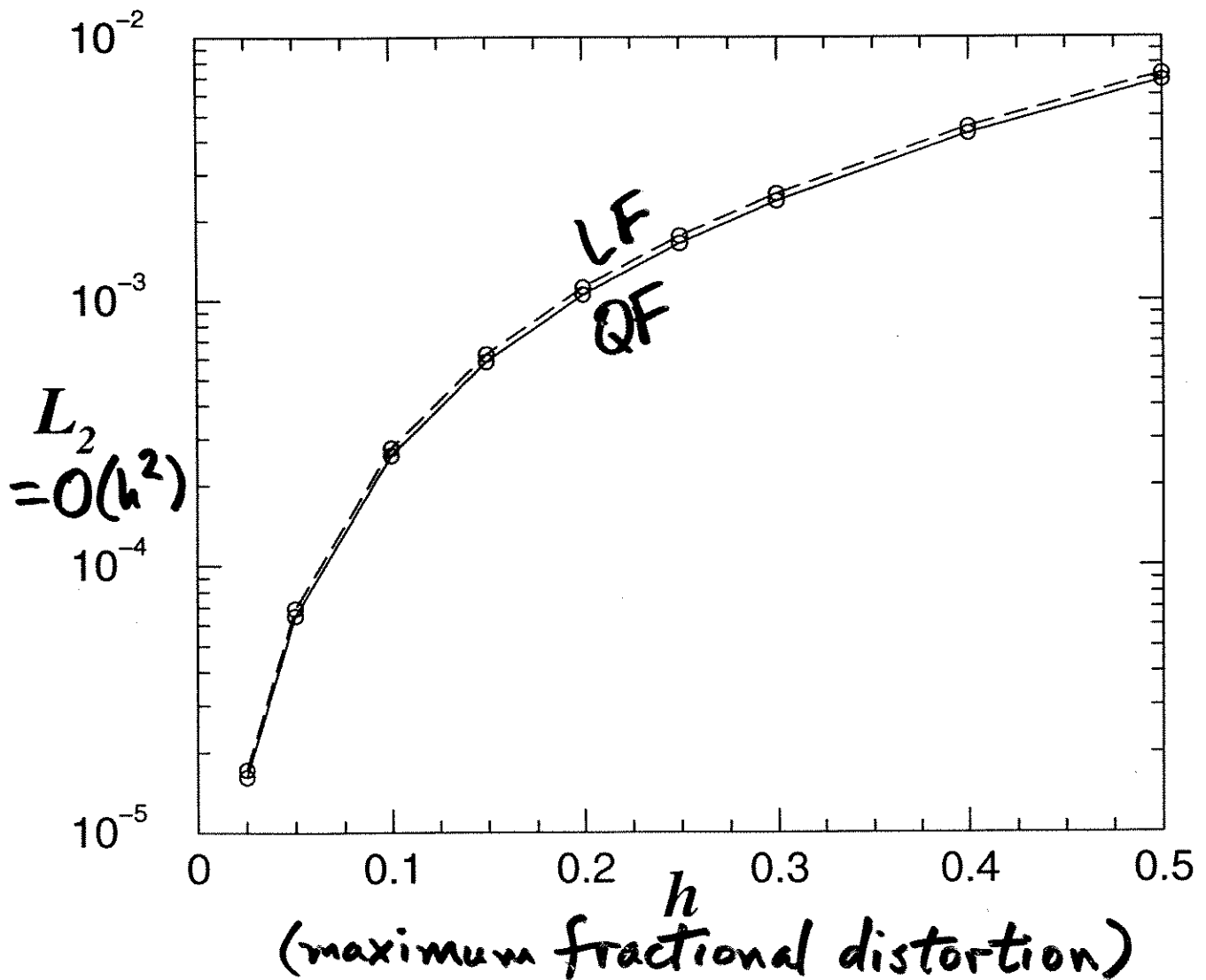


Figure 1: Numerical results from John Wilson

Uniform flow
Planar primary interior faces
All runs $8 \times 8 \times 8$



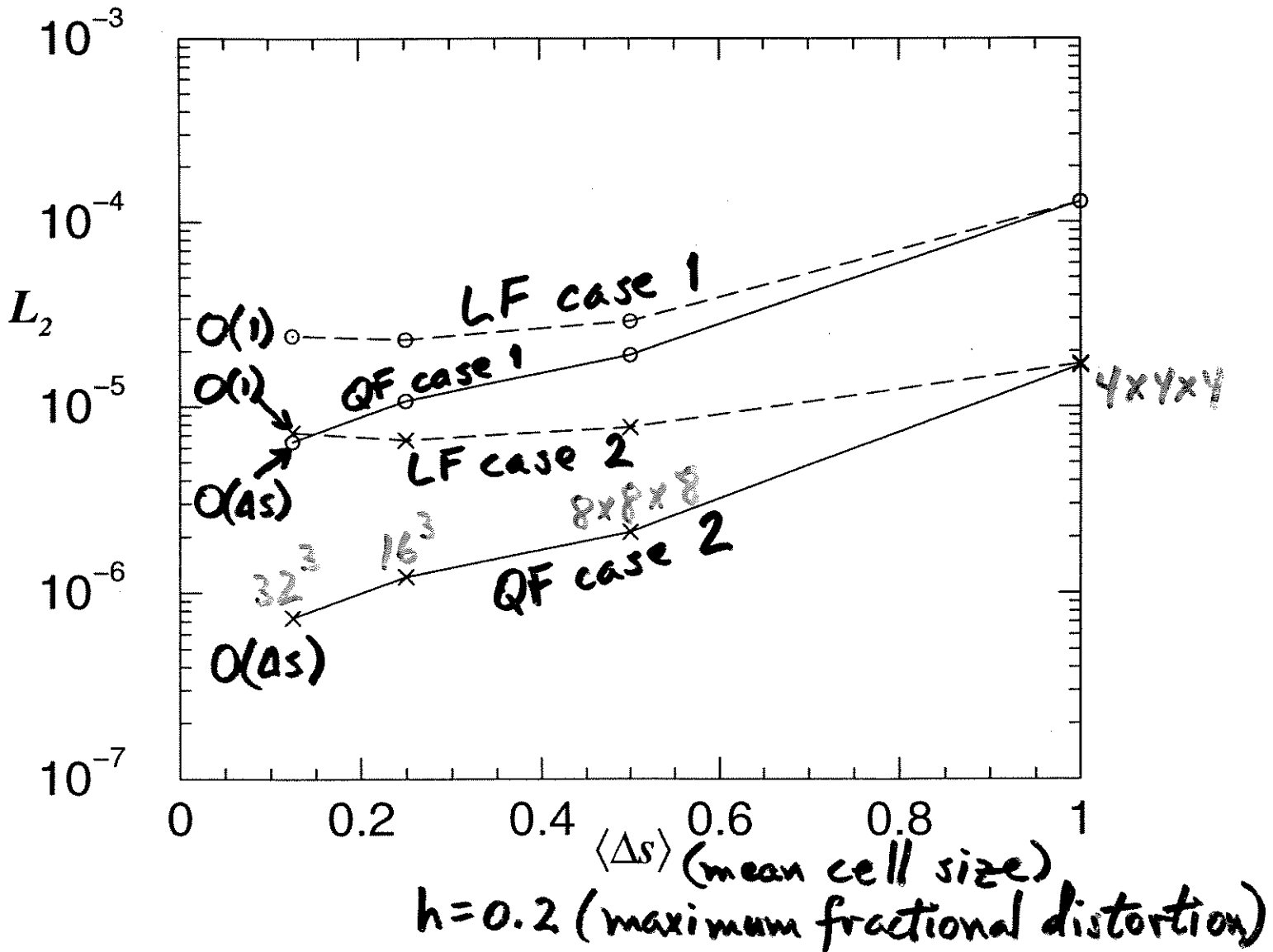
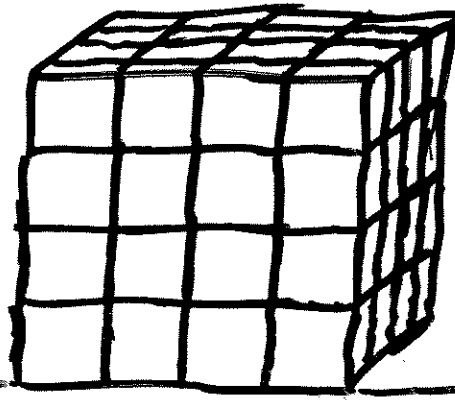
Uniform flow
Random (non-planar) primary interior faces
All runs $8 \times 8 \times 8$

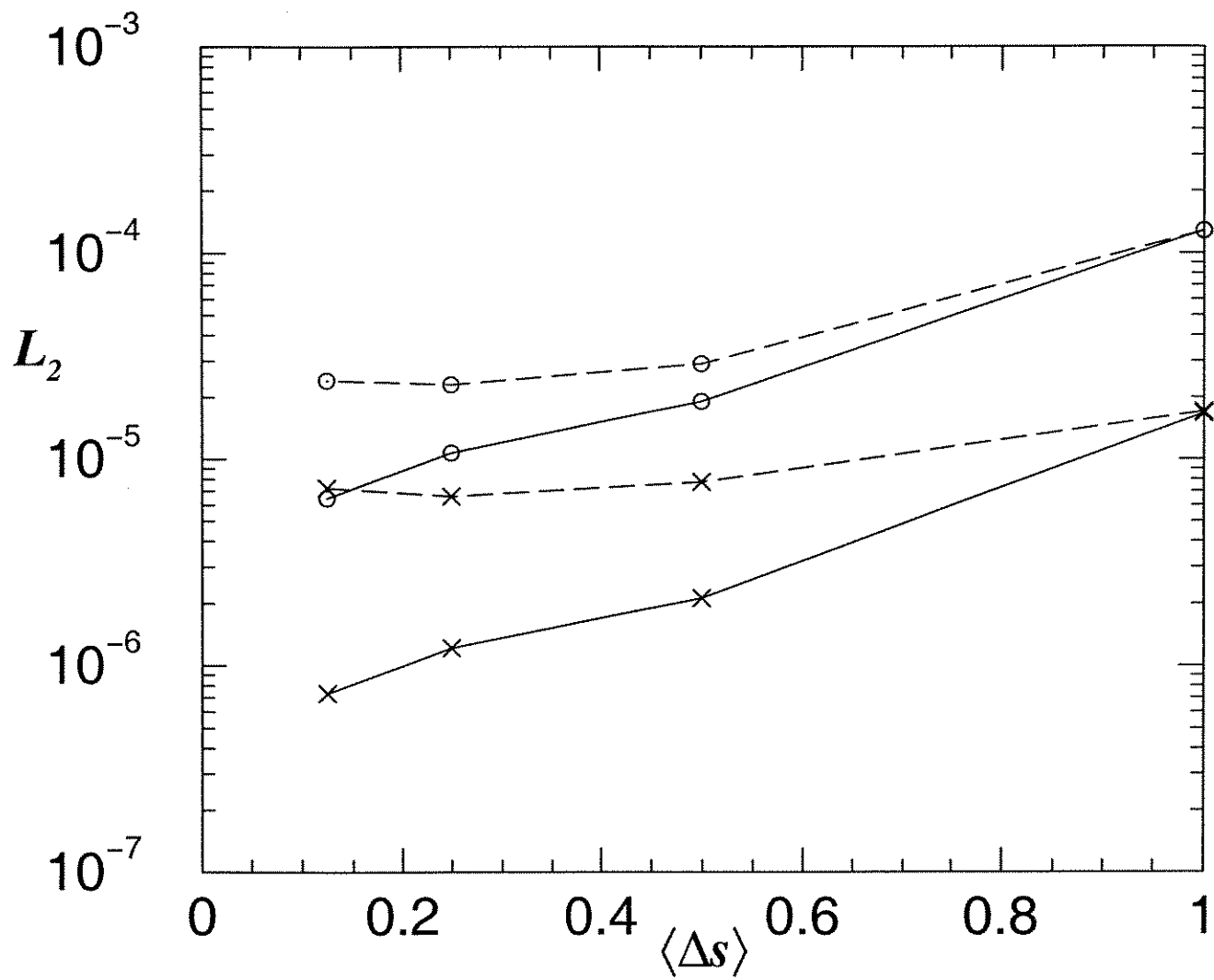


Non-uniform flow

Homogeneous
Planar primary
interior faces

Random
refinement



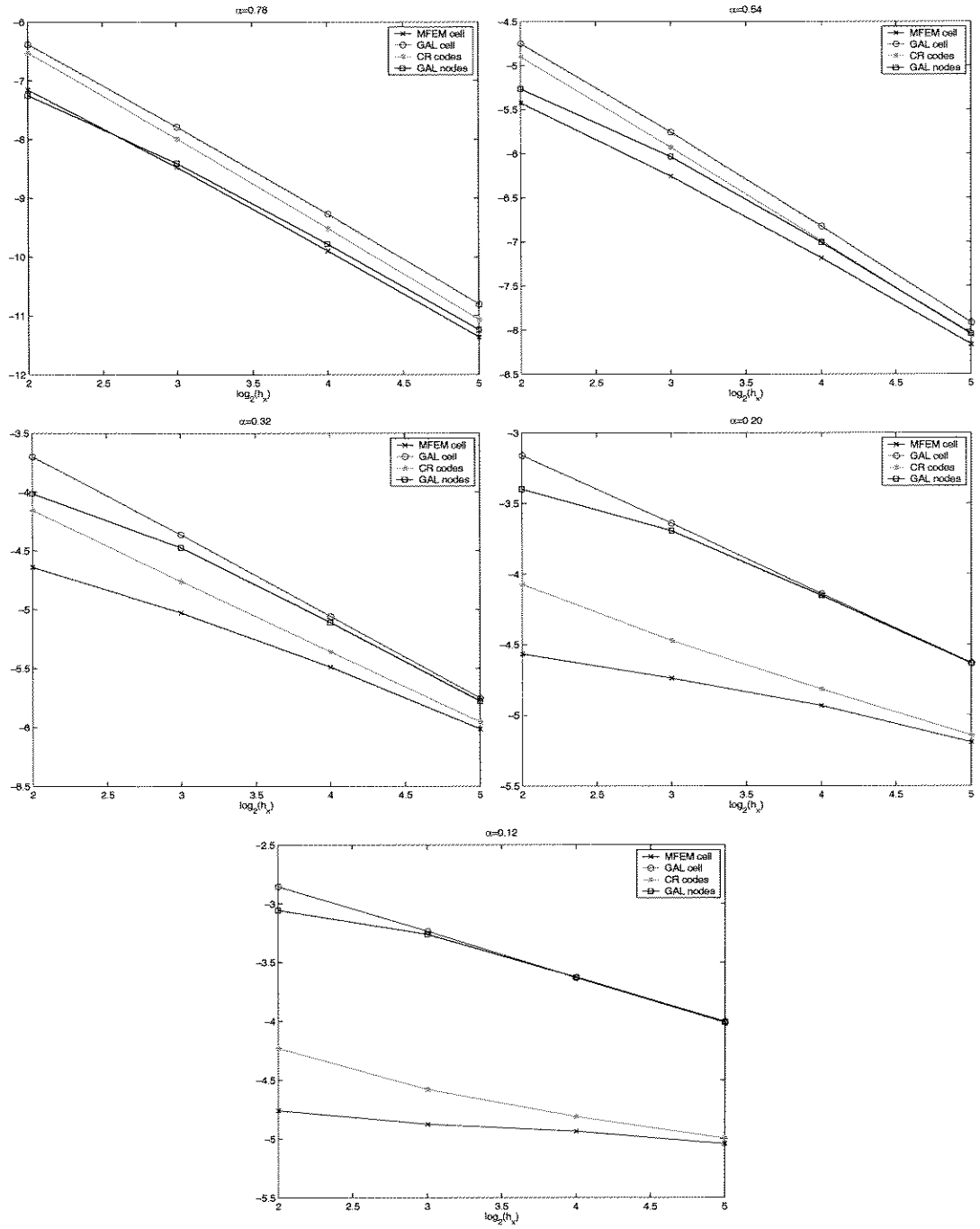


Solutions with Singular Velocities

- Checkerboard scalar \mathbf{K} on 2×2 coarse grid
- p like r^α near the origin (center of grid), $p \in H^{1+\alpha-\epsilon}$
- Grid: squares divided into two right triangles
- GAL = standard C^0 linears, expect $h^{2\alpha-\epsilon}$ for p
- CR = Crouzeix-Raviart
- Discrete L^2 p error at centroids (CR = MFEM \mathbf{RT}_0) or nodes
- Discrete CR velocity = MFEM \mathbf{RT}_0 velocity (cf. Marini 1985)
- Discrete L^2 v error at centroids

Convergence rates

\mathbf{K} ratio	α	CR p	GAL p	CR v	GAL v
1/2	0.78	1.47	1.50	0.7347	0.7498
1/5	0.54	1.06	1.04	0.5401	0.5577
1/15	0.32	0.60	0.67	0.3242	0.4035
1/40	0.20	0.33	0.48	0.1440	0.3095
1/100	0.12	0.18	0.37	0.0262	0.2453



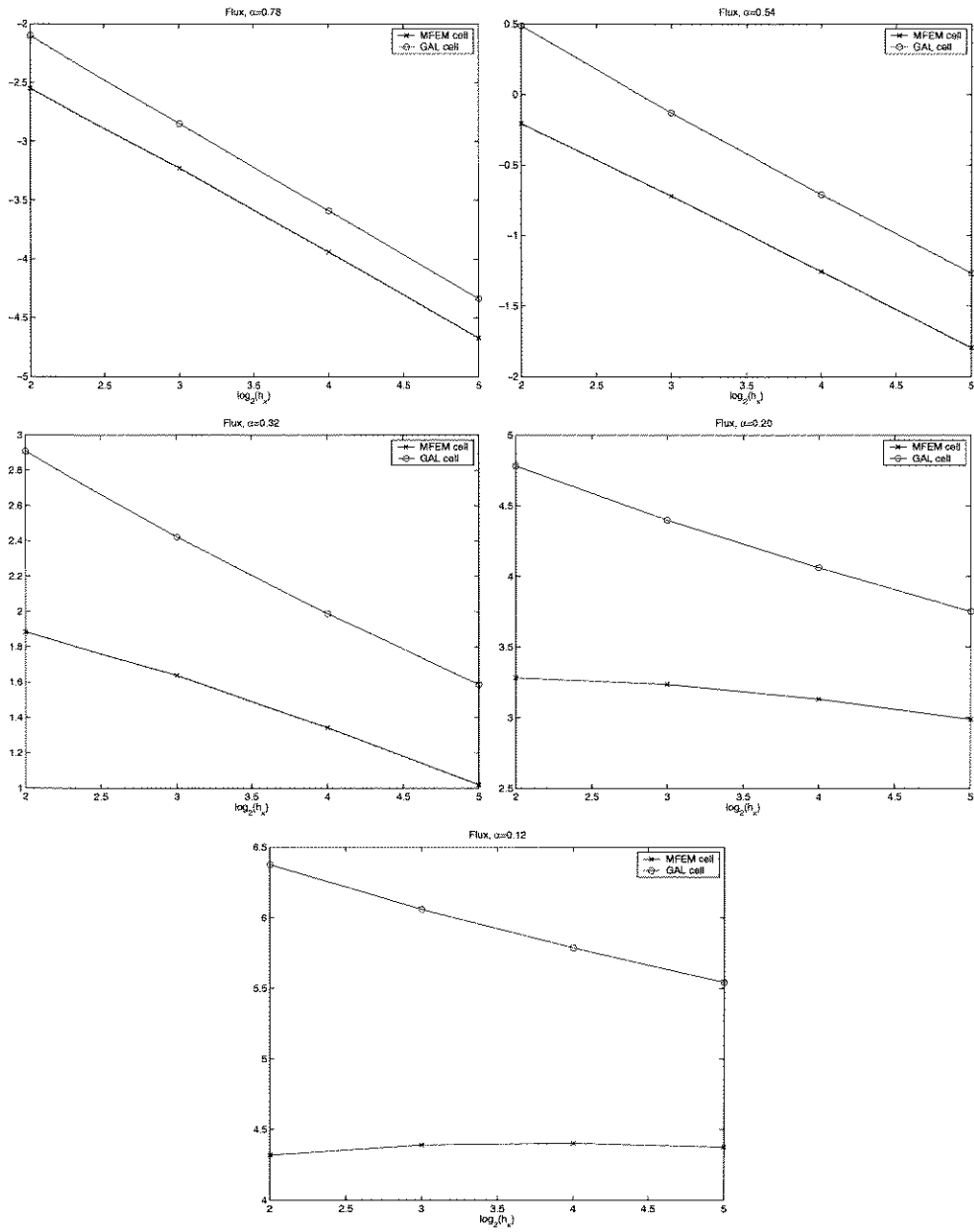


Figure 3: Log2 velocity convergence plot of Galerkin FEM vs. MFEM with RT_0 element in a discrete L2 norm.

Conclusions

- The relation between the methods is:
 - * built on the common continuous flux and “weak” continuous pressure.
 - * important in understanding behavior of methods for discontinuous permeability or on an irregular grid.
- “Weakly” continuous pressure \implies the need for Lagrange multipliers is eliminated.
- Methods can be grouped into \mathbf{K} methods and \mathbf{K}^{-1} methods. \mathbf{K}^{-1} methods appear to be more robust on “nasty” grids.
- A rigorously consistent “compatible” 3D method with small stencil for general distorted hexahedra is difficult to construct.
- Need more testing of various methods for cases of singular velocities. Compatibility appears to be a virtue.

References

(links at <http://www-math.cudenver.edu/~trussell>)

- R.A. Klausen and T.F. Russell,
Relationships among some locally conservative discretization methods which handle discontinuous coefficients,
<http://www-math.cudenver.edu/ccm/reports/rep203.ps.gz>;
Computational Geosciences, submitted.
- R.L. Naff, T.F. Russell, and J.D. Wilson,
Shape functions for velocity interpolation in general hexahedral cells,
Computational Geosciences, **6** (2002), 285–314.
- R.L. Naff, T.F. Russell, and J.D. Wilson,
Shape functions for three-dimensional control-volume mixed finite-element methods on irregular grids,
<http://www-math.cudenver.edu/ccm/reports/rep183.ps.gz>.